

# Assessment of developed IMRT and 3D-CRT planning protocols for treating nasopharyngeal cancer patients based on the target and organs at risks common volumes

Gh. Sharbo<sup>1</sup>, B. Hashemi<sup>1\*</sup>, M. Bakhshandeh<sup>2</sup>, A. Rakhsha<sup>3</sup>

<sup>1</sup>Department of Medical Physics, Faculty of Medical Sciences, Tarbiat Modares University, Tehran, Iran

<sup>2</sup>Department of Radiology Technology, Faculty of Allied Medical Sciences, Shahid Beheshti University of Medical Sciences, Tehran, Iran

<sup>3</sup>Department of Radiation Oncology, Faculty of Medical Sciences, Shahid Beheshti University of Medical Sciences, Tehran, Iran

## ABSTRACT

### ► Original article

#### \*Corresponding author:

Bijan Hashemi Malayeri, Ph.D.,

#### E-mail:

bhashemi@modares.ac.ir

Received: September 2020

Final revised: March 2021

Accepted: April 2021

Int. J. Radiat. Res., April 2022;  
20(2): 307-315

DOI: 10.52547/ijrr.20.2.8

**Keywords:** Nasopharyngeal carcinoma, intensity modulated radiation therapy, 3D radiation therapy, treatment planning, radiobiological models.

**Background:** Various developed intensity modulated radiation therapy (IMRT) and a three dimensional conformal radiation therapy (3D-CRT) protocols were assessed for treating nasopharyngeal cancer (NPC) based on radiobiological parameters. **Materials and Methods:** Treatment plans were made for 30 NPC patients using 15 developed IMRT and 3D-CRT protocols. The IMRT protocols comprised of three 7-fields with various collimator (0°, 5°, and 10°) and couch (0°, 4°, 8°, 12°) angles. The 3D-CRT technique included two phases. In the 1st phase a dose of 60 Gy was prescribed to the total PTV, but in the 2nd phase a dose of 10 Gy was prescribed to the PTV-70. The tumour control probability (TCP), normal tissues complication probability (NTCP), and complication-free tumor control probability (P+) parameters were estimated for assessing the IMRT protocols. Then, the ideal protocol (s) were proposed through comparing the IMRT protocols with each other and 3D-CRT protocol based on TCP, NTCP, and P+ values. **Results:** The IMRT protocol with 10° collimator and 8° couch angles had the lowest NTCP mean values. Significant differences were observed among the mean NTCP values for the brainstem and parotid glands, and P+ of the developed IMRT and 3D-CRT protocols. However, no significant differences were observed among the mean NTCP values for the spinal cord, optic chiasm and optic nerves among the protocols. **Conclusions:** The 3D-CRT protocol had a good outcome for the NPC patients having a lower common volume between their total planning target volume and OARs, while the results of the IMRT showed the opposite.

## INTRODUCTION

Nasopharyngeal cancer (NPC) is a pathological, epidemiological and clinical entity distinct from other head and neck cancers, and one of the most common malignant tumors in the world, with the highest incidence occurring in the southern China, southeast Asia, middle east and north Africa <sup>(1, 2)</sup>. Radiation therapy concurrently with chemotherapy is the definitive treatment for NPC <sup>(3, 4)</sup>. IMRT provides improved tumor target coverage with significant sparing of sensitive normal tissue structures in the treatment of NPC. Randomized trials have shown a reduction in late xerostomia, resulting in an important improvement in the quality of life with IMRT compared with CRT <sup>(5-7)</sup>.

In NPC radiotherapy, vital structures (such as: the salivary glands, brainstem, spinal cord, optic nerves and optic chiasm) are close to the tumor volumes. IMRT provides sharp dose gradients between the

margins of target volumes and organs at risk (OARs). For 3D-CRT, different techniques have also been proposed to spare the spinal cord <sup>(8-13)</sup>. By the way, these techniques are faced with the problem of field matching leading to either uncontrolled fields overlap or gap at the level of the planning target volume (PTV) or OAR complications. Some studies <sup>(14-16)</sup> have also been done comparing 3D-CRT and IMRT plans for nasopharyngeal cancer using radiobiological modeling. Nevertheless, such studies have not proposed any optimal treatment plans through considering radiological parameters (such as TCP and NTCP) and anatomical relationships between the target and OARs for NPC patients.

Furthermore, all previous studies have used only the traditional IMRT and 3D-CRT planning procedures and have not reported the complication free tumor control probability (p+). In our previous study <sup>(17)</sup> 11, non-traditional novel IMRT protocols were developed for treatment planning of a group of

NPC patients using various linac collimator angles and non-coplanar fields. In that study, relative sterility (RS) and Poisson models were used for calculating the mean values of dosimetric and radiobiological parameters and the effect of increasing the couch angle (up to 12 degree) was investigated as the NPC treatment area is very small and includes vital organs. However, using IMRT planning for NPC remains challenging due to its' complex anatomy including bones, soft tissues and air cavities all needing special consideration. In addition, the NPC targets are prescribed with different dose levels <sup>(18)</sup> and their volumes have often irregular concave shapes <sup>(19)</sup>.

Moreover, treatment planning of IMRT procedures demands lots of time and adaptive strategies enforcing investigators to develop them. These bring about both additional cost to patients and extra work load to clinical staff. To overcome the limitations of previous studies, in this research plus 11 novel IMRT protocols developed before <sup>(17)</sup>, 4 additional novel IMRT protocols as well as a specific 3D-CRT protocol were developed and performed for the treatment of NPC patients and their relevant radiobiological parameters were estimated. Then, the ideal IMRT/3D-CRT protocol (s) was selected and proposed based on the analyses of estimated TCP, NTCP and P+ values for treating NPC patients with different ranges of common volumes between their target and OARs.

Our study provided a new assessment procedure that can be adopted for selecting and implementing appropriate IMRT/3D-CRT treatment planning protocol for NPC patients. Our proposed procedures are based on fitting and shielding the spinal cord, reducing OARs doses, providing optimal target coverage, and avoiding beam junctions.

## MATERIALS AND METHODS

### *Patient characteristics*

Thirty NPC patients consisting of 24 males and 6 females with an age ranging from 18 to 67 years who underwent radical IMRT and 3D-CRT were selected for this study. The patients were at early and advanced NPC stages (from stage I to IV). All the patients had the diagnostic computed tomography (CT) (Siemens Medical Solutions USA, Inc., Emotion Model, with slice thickness: 3-5 mm, matrix size: 512\*512) as well as magnetic resonance (MR) (Siemens Medical Solutions USA, Inc., Avanto Model, with magnetic field strength: 1.5T, TE: 100ms and TR: 3000ms) scans. A thermoplastic mask was used for immobilization of the patients. The patients' anatomic contours were delineated on the fused CT and MR images using the Eclipse version 6.5 software (Varian Medical Systems Inc., USA).

### *Target and OAR definition*

Target volumes (GTV, CTV, PTV) were delineated based on the recommendations proposed by Radiation Therapy Oncology Group (RTOG-0615) <sup>(20)</sup> using the Eclipse treatment planning system (Eclipse TPS, version 13, Varian Company, USA) of a 6 MV Varian linac. A dose of 70 Gy was used for treating the patients' nasopharyngeal primary and gross nodal disease and its' required margins denoted as the planning target volume of 70 (PTV-70). Additionally, a dose of 59.4 (PTV-59.4) and 54 Gy (PTV-54) were applied for the high- and low-risk lymph nodes, respectively. For all the PTVs, a 5-mm margin was added to the clinical target volumes by the radiation oncologist, except in the areas adjacent to the critical structures.

Critical normal structures identified as OARs were also contoured and expanded according to the RTOG-0615 <sup>(20)</sup>, including the brain stem, spinal cord, optic nerves, optic chiasm and parotid glands, on each CT slice, by the treatment planning team.

### *IMRT treatment plans*

In addition to 11 novel IMRT protocols developed before <sup>(17)</sup> with various collimator and couch angles, 4 additional protocols were developed and performed for all the NPC patients. The additional protocols were all 7-field IMRT plans comprised of a combination of 2+5 fields with 5° and 0° collimator angle respectively and 12° couch angle (Protocol 6), another 2+5 fields with 10° and 0° collimator angle respectively and 12° couch angle (protocol 9), a 5+2 fields with 5° and 0° collimator angle respectively and 12° couch angle of (protocol 12), and finally another 5+2 fields with 10° and 0° collimator angle of and 12° couch angle (protocol 15). Details of these extra protocols and all the previous protocols are described in table 1. The prescribed dose used for all the plans was 70 Gy to the 95% isodose of the PTV, in 33 fractions of 2.12 Gy. All the plans were normalized in such a way that at least 95% of the PTV is covered by the prescribed dose. The volume of the PTV receiving more than 110% and less than 93% of the prescribed dose did not exceed 20% and 1%, respectively.

No more than 110% of the prescribed dose was outside the PTV. The dose received by each OAR was limited to the recommended dose constraints proposed by the RTOG-0615 <sup>(20)</sup>. Dose volume histograms (DVH) were generated for each plan, and the PTV dose coverage and OAR dosimetry were used for estimating the radiobiological parameters and evaluating the treatment plans.

### *3D-CRT treatment plans*

The 3D-CRT technique used in this study included two phases as follows. In the first phase a dose of 60 Gy was prescribed to the total PTV. This consisted of

a completely isocentric technique with five photon beams (fields) as illustrated in figure 1. The beams consisted of two long lateral fields as seen in figure 1 (a) (with the gantry angles of 90° and 270°) covering all of the PTV, including the spinal cord that could be kicked out by turning the couch away from the collimator by about 5–15° and turning the gantry versus the anterior position by about 5–15° to reach a better dose distribution; plus a posterior field as shown in figure 1(b) (gantry angle 180°) with a block shielding the spinal cord; and finally two symmetrical fields as seen in figure 1(c) with a posterior obliquity at the gantry angles of 210–220° and 140–150° from the right and left sides, respectively. Shielding blocks were used for sparing the spinal cord and also covering part of the PTV (all the left side on the beam's-eye view (BEV) for the right posterior field and all the right side for the left posterior field), as seen in figure 1.

All the fields had individually-shaped blocks conformed to the PTV contour. The arrangement of spinal cord shielding blocks was drawn to cover at least 6-mm safety margin in the BEV. Wedges were used whenever necessary. Beams were weighted to conform the dose distribution for achieving the dose requirements and constraints. The beam weights were set in the range of 27.5–29.2% for each of the two first lateral fields, 6.5–7.5% for the posterior field, and 17.5–18.5% for each of the final two posterior oblique fields.

In the second phase the PTV-59.4 and PTV-54 were deleted and a dose of 10 Gy was prescribed to the PTV-70. Then, the same technique (as described above) was applied.

### Evaluation of radiobiological parameters using Biosuite software

Biosuite<sup>(21)</sup> is a user-friendly software facilitating the biological evaluation of treatment plans. The input data for the Biosuite is differential DVH data, obtained from treatment planning system (TPS). The Biosuite utilizes the dose prescribed to the target volume, irradiated volume, normalized percentage for the TCP and NTCP calculation, as well as minimum, maximum, and average dose to the PTV. The biological parameters of the tumor ( $\alpha$  and  $\alpha/\beta$ ) and clonogenic density (the number of clonogenic cells/cm<sup>3</sup>) are also used for calculating the TCP through the Biosuite. The basic equation of the TCP utilizes the Poisson statistical model according to which the probability of the occurrence of N number of a particular event is defined in equation (1):

$$P(n) = [\exp(-a) * (a)^n] / n! \quad (1)$$

Where; “a” is a positive real number equal to the expected number of occurrences happening during the given interval. From the radiobiological point of view, equation (1) can be modified as shown in

equation (2):

$$(n) = [\exp(-N_s) * (N_s)^n] / n! \quad (2)$$

Where;  $N_s$  is the expected number of cells survived during the given interval after an exposure to dose D (Gy) and n is the actual number of the survived cells. For complete tumor treatment (i.e.,  $n > 4$ ), the final equation of the TCP could be obtained from equation (3):

$$TCP(n=0) = \exp(-N_s) \quad (3)$$

The Biosuite uses the differential DVH data of TPS; in other words, it counts for each and every dose bin which depends on the physical and dosimetric properties of the treatment unit. We calculated the NTCP for brainstem, spinal cord, optic chiasm, optic nerves and parotid glands using the relative seriality model with the Biosuite software. With this model the binomial statistics is used to obtain the probability of the damage to normal tissue (s) or NTCP accounting for the serial and parallel architecture of the functional subunits as expressed in equation (4):

$$NTCP = \left[ 1 - \prod_{j=1}^k (1 - NTCP(D_j)^s)^{v_j} \right]^{1/s} \quad (4)$$

The formula describes the response of the whole organ to an arbitrary dose distribution ( $D_j, v_j$ ) as a function of the response of the whole organ to a homogeneous dose distribution. The number of functional subunits has been made to coincide with the k bins in the DVH, where “s” is the relative seriality factor. NTCP ( $D_j$ ) can therefore be expressed as expressed in equation (5):

$$NTCP(D_j) = 2^{-s \cdot \gamma \cdot \left(1 - \frac{D_j}{D_{50}}\right)} \quad (5)$$

The Biosuite has a library of s,  $\gamma$ , and  $D_{50}$  values for brainstem, spinal cord, optic chiasm, optic nerves and parotid glands<sup>(22)</sup>.

The effectiveness of different treatment plans used in our study were also evaluated by the radiobiological concept of complication-free tumor control probability (P+) representing the probability of achieving tumor control without causing damage to normal tissues<sup>(23)</sup>. The P+ index can be calculated by equation (6):

$$P+ = TCP - NTCP \quad (6)$$

### Statistical analysis

Statistical analyses were performed for all the parameters of interests acquired for all the 15 IMRT as well as the 3D-CRT protocols implemented on all the NPC patients using the Statistical Package for Social Science (SPSS) software (SPSS Version 17 for

Windows, IBM SPSS Statistics, USA). All the acquired data is expressed by mean±standard deviation. The analysis of variance with repeated measures was used for comparing the groups and the p-values less than 0.05 were considered as statistically significant.

**Table 1.** Details of the IMRT planning protocols implemented for treating the NPC patients.

Protocols	Treatment fields and collimator angle (in°) combination	Couch angle (in°)
1	7 Fields with collimator angle of 0	0
2	7 Fields with collimator angle of 5	0
3	7 Fields with collimator angle of 10	0
4	2+5 fields with collimator angle of 5 and 0 respectively	4
5	2+5 fields with collimator angle of 5 and 0 respectively	8
6	2+5 fields with collimator angle of 5 and 0 respectively	12
7	2+5 fields with collimator angle of 10 and 0 respectively	4
8	2+5 fields with collimator angle of 10 and 0 respectively	8
9	2+5 fields with collimator angle of 10 and 0 respectively	12
10	5+2 fields with collimator angle of 5 and 0 respectively	4
11	5+2 Fields with collimator angle of 5 and 0 respectively	8
12	5+2 fields with collimator angle of 5 and 0 respectively	12
13	5+2 fields with collimator angle of 10 and 0 respectively	4
14	5+2 fields with collimator angle of 10 and 0 respectively	8
15	5+2 fields with collimator angle of 10 and 0 respectively	12

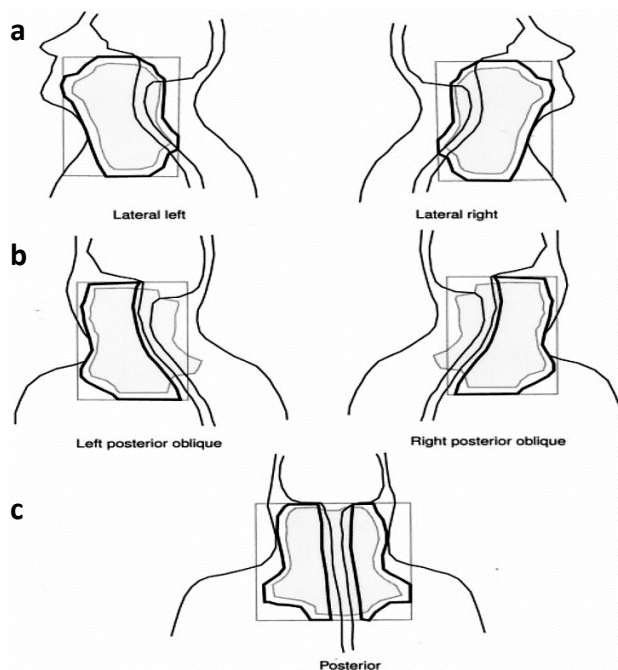


**Figure 1.** Five-field technique in BEV drawings. Thick lines represent the irradiation field, the beam edges are the rectangular grey lines. PTV is the grey area, patient contour and spinal cord are outlined.

## RESULTS

The mean, maximum and minimum volumes for total planning target volume (TPTV) and OARs are presented in table 2. All the patients had a noticeable feature of having a common volume between their TPTV and parotids glands.

### Evaluation of IMRT protocols

#### Analyses of the TCP, NTCP and P+

For the TCP, NTCP and P+ analysis, all the 15 various IMRT protocols showed a strong correlation with only one parameter, namely the common volume between the TPTV and OARs. For performing statistical analysis on the data, the total range of the common volumes were divided into three ranges including: "0 to 6", "6 to 12" and "≥12" cm<sup>3</sup>.

The TCP means calculated based on the Poisson model from the NPC patients' data for all the IMRT protocols are presented in table 3. Analysis of the TCP values showed no statistically significant differences ( $p>0.05$ ) among the various IMRT protocols used in our study.

The calculated NTCP mean values derived based on the relative seriality model from all of the OARs (brainstem, spinal cord, optic chiasm, optic nerves and parotid glands) are presented in table 4. Analysis of the NTCP values indicated statistically significant difference ( $p=0.0001$ ) between the IMRT protocols for lower range (0 to 6 cm<sup>3</sup>) of the common volume between TPTV and OARs, but no statistically significant differences ( $p>0.05$ ) were noted for higher ranges (6 to 12 cm<sup>3</sup> and  $\geq 12$  cm<sup>3</sup>). However, for lower range (0 to 6 cm<sup>3</sup>) of the common volume the least mean NTCP value was achieved with the IMRT protocol 14 (5+2 fields with a collimator angle of 10° and 0° and a couch angle of 8°).

The calculated mean of P+ values for all the IMRT protocols are presented in table 5 showing no statistically significant differences ( $p>0.05$ ) between the IMRT protocols.

All the other IMRT protocols (nos. 1-13 and 15) were also compared with protocol 14 for lower common volume range (0 to 6 cm<sup>3</sup>) between the TPTV and OARs using the repeated measurement analysis. The significant levels (p-values) of the IMRT protocol 14 compared to other protocols are presented in table 5. As can be seen from the table, the resulting p-values indicate that the NTCP mean values of the IMRT protocol 13 (5+2 fields with a collimator angle of 10° and 0° and a couch angle of 4°) is very close ( $p=0.993$ ) to that of protocol 14.

### Evaluation of the IMRT and 3D-CRT protocols

Statistical analysis of the data acquired from 15 various developed IMRT protocols indicated a significant difference regarding the NTCP mean for protocol 14 compared to other protocols for lower



range (0 to 6 cm<sup>3</sup>) of the common volume between the TPTV and OARs. Therefore, at the next steps we just compared the results of the IMRT protocol 14 with the common 3D-CRT protocol for which a strong correlation was noted only for the common volumes between the TPTV and OARs parameters.

### Mean dose to the OARs

Table 6 shows the mean and standard deviation values of  $D_{\text{mean}}$  doses received by the brainstem, spinal cord, optic chiasm, optic nerves, parotid glands and PTV using the IMRT and 3D-CRT protocols. In general, the doses to the OARs and PTV were achieved based on the dose criteria recommended by the RTOG-0615 (20). Comparison of the IMRT protocol 14 with 3D-CRT protocol indicated statistically significant differences for some organs including the brainstem, spinal cord, and parotid glands. For the brain steam and spinal cord, the 3D-CRT had the least mean of  $D_{\text{mean}}$  values of  $17.26 \pm 1.31$  Gy ( $p < 0.001$ ) and  $14.54 \pm 1.37$  Gy ( $p < 0.001$ ) respectively. By the way, for the parotid glands, the IMRT protocol had the least mean of  $D_{\text{mean}}$  value of  $32.55 \pm 1.12$  Gy ( $p < 0.001$ ) compared with the 3D-CRT protocol. For other organs, including the optic chiasma, optic nerves and PTV, no statistically significant differences were observed among the mean of  $D_{\text{mean}}$  values of the IMRT and 3D-CRT protocols ( $p > 0.05$ ).

### Analyses of TCP, NTCP and P+

The calculated NTCP mean values derived from all of the OARs (brainstem, spinal cord, optic chiasm, optic nerves and parotid glands) are presented in table 7. As can be seen in the table, the data presented for brainstem shows statistically significant difference ( $p = 0.035$ ) between the IMRT protocol 14 and 3D-CRT protocol for the highest range ( $\geq 12$  cm<sup>3</sup>) of the common volume between the TPTV and OARs, while there are no statistically significant differences ( $p > 0.05$ ) between the IMRT and 3D-CRT protocols for other ranges (0 to 6 and 6 to 12 cm<sup>3</sup>). However, the IMRT shows the least NTPC mean values for all ranges of the common volume. For other organs, including the spinal cord, optic chiasm and optic nerves, no statistically significant differences ( $p > 0.05$ ) are observed among the NTCP mean values of the IMRT and 3D-CRT protocols. On the other hand, for parotid glands, there is statistically significant difference ( $p < 0.05$ ) between the IMRT and 3D-CRT protocols with the IMRT showing the least NTPC mean values for all ranges of the common volume between the TPTV and OARs (figure 2).

Table 8 presenting the calculated TCP mean values derived from all of the PTVs indicates no statistically significant difference between the IMRT and 3D-CRT protocols for all ranges of the common volume between the TPTV and OARs (figure 3b). But, regarding the mean of TNTCP and P+ values,

statistically significant differences are observed between the IMRT and 3D-CRT protocols ( $p < 0.05$ ). The IMRT protocol shows lower NTCP and higher P+ mean values for all ranges of the common volume with a direct and inverse relationship between the NTCP and P+ mean values and the common volumes, respectively (figure 3a, 3c).

**Table 2.** The mean, minimum, maximum and standard deviation (SD) of the patients' OARs, TPTV and the common volumes (in cm<sup>3</sup>) between TPTV and parotids glands.

OARs	V <sub>min</sub>	V <sub>max</sub>	V <sub>mean</sub> ±SD
Brain steam	14.3	40.2	23 ± 5.27
Spinal cord	8.2	55.9	25.57 ± 13.36
Optic chiasm	0.1	0.9	0.63 ± 0.34
Optic nerves	0.1	1.4	0.45 ± 0.35
Parotid glands	3.95	45	22.58 ± 10.95
TPTV	182.2	2014.7	987.27 ± 326.8
Common volume	0	23.1	8.26 ± 6.44

**Table 3.** The mean of TCP ± SD % values calculated from the NPC patients' data for the 15 developed IMRT protocols based on Poisson model for different ranges of the common volume between the TPTV and OARs with relevant p-values

IMRT Protocols	Mean TCP for different ranges of the common volume ± SD %		
	0 – 6 (cm <sup>3</sup> )	6 – 12 (cm <sup>3</sup> )	≥ 12 (cm <sup>3</sup> )
1	94.40 ± 1.73	94.28 ± 2.06	92.75 ± 1.69
2	94.17 ± 1.96	93.33 ± 2.91	93.64 ± 1.35
3	94.29 ± 1.99	95.56 ± 0.78	93.25 ± 1.81
4	93.74 ± 1.81	94.55 ± 1.39	94.55 ± 1.31
5	93.82 ± 1.88	96.10 ± 0.56	94.51 ± 1.31
6	93.70 ± 1.81	96.2 ± 0.60	94.55 ± 1.29
7	92.71 ± 2.74	95.70 ± 0.63	94.50 ± 1.24
8	92.90 ± 2.72	94.30 ± 1.92	94.35 ± 1.26
9	92.88 ± 2.75	94.45 ± 1.82	94.33 ± 1.20
10	93.91 ± 1.93	95.78 ± 0.56	94.18 ± 1.39
11	93.81 ± 2.06	95.82 ± 0.58	93.96 ± 1.43
12	93.85 ± 2.04	95.85 ± 0.6	93.86 ± 1.45
13	94.36 ± 1.71	94.55 ± 1.43	92.38 ± 1.95
14	94.14 ± 1.82	94.28 ± 1.47	92.01 ± 2.16
15	94.16 ± 1.85	94.29 ± 1.45	92 ± 2.14
p-value	0.774	0.799	0.2

**Table 4.** The mean of NTCP ± SD % values calculated from the NPC patients' data for the 15 developed IMRT protocols based on the relative sterility model for different ranges of the common volume between the TPTV and OARs with relevant p-values.

IMRT Protocols	Mean NTCP for different ranges of the common volume ± SD %		
	0 – 6 (cm <sup>3</sup> )	6 – 12 (cm <sup>3</sup> )	≥ 12 (cm <sup>3</sup> )
1	20.19 ± 2.92	40.61 ± 5.42	43.88 ± 4.70
2	19.86 ± 3.16	39.65 ± 5.54	43.68 ± 5.22
3	20.50 ± 3.09	39.36 ± 5.25	44.08 ± 5.17
4	19.28 ± 2.88	40.06 ± 5.29	45.51 ± 4.90
5	19.27 ± 3.02	39.89 ± 5.33	45.40 ± 4.93
6	19.46 ± 3.02	39.9 ± 5.33	45.41 ± 4.93
7	19.65 ± 2.87	40.25 ± 5.29	46.30 ± 4.57
8	19.66 ± 3.00	40.07 ± 5.37	46.59 ± 4.51
9	19.83 ± 3.00	40.08 ± 5.37	46.6 ± 4.51
10	19.33 ± 2.97	40.02 ± 5.33	45.07 ± 4.65
11	19.32 ± 2.95	39.55 ± 5.21	45.17 ± 4.62
12	19.50 ± 2.92	39.56 ± 5.21	45.18 ± 4.62
13	18.49 ± 2.87	40.12 ± 5.25	44.89 ± 4.72
14	18.48 ± 2.88	40.03 ± 5.23	44.09 ± 4.97
15	18.68 ± 2.88	40.04 ± 5.23	44.1 ± 4.97
p-value	0.0001	0.274	0.417

**Table 5.** The mean values of P+  $\pm$  SD calculated from the NPC patients' data for 15 developed IMRT protocols for different ranges of the common volume between the TPTV and OARs with relevant p-values and relationships of protocol 14 with other protocols with relevant p-values

IMRT Protocols	Mean P+ for different ranges of the common volume $\pm$ SD %			Relationships of protocol 14 with other IMRT protocols using repeated measurement analysis with relevant p-values	
	0 – 6 (cm <sup>3</sup> )	6 – 12 (cm <sup>3</sup> )	$\geq$ 12 (cm <sup>3</sup> )		
1	74.20 $\pm$ 3.52	53.67 $\pm$ 5.18	48.87 $\pm$ 5.09	Protocol no. 1 2 3 4 5 6 7 8 9 10 11 12 13 15	P-value 0.056 0.016 0.007 0.089 0.15 0.05 0.004 0.006 0.003 0.002 0.04 0.006 0.993 0.001
2	74.35 $\pm$ 4.34	53.62 $\pm$ 5.28	50.25 $\pm$ 5.62		
3	74.14 $\pm$ 3.95	56.31 $\pm$ 5.25	48.84 $\pm$ 5.99		
4	74.44 $\pm$ 3.81	54.49 $\pm$ 5.18	54.9 $\pm$ 49.03		
5	74.57 $\pm$ 4.16	56.20 $\pm$ 5.30	49.10 $\pm$ 5.49		
6	74.45 $\pm$ 3.83	54.48 $\pm$ 5.17	49.02 $\pm$ 5.45		
7	72.24 $\pm$ 4.77	55.45 $\pm$ 5.29	48.35 $\pm$ 5.20		
8	72.32 $\pm$ 4.97	54.22 $\pm$ 5.81	47.76 $\pm$ 5.10		
9	72.25 $\pm$ 4.87	55.47 $\pm$ 5.4	48.37 $\pm$ 5.15		
10	74.47 $\pm$ 4.20	55.76 $\pm$ 5.33	49.22 $\pm$ 5.38		
11	74.67 $\pm$ 4.33	56.27 $\pm$ 5.26	48.89 $\pm$ 5.30		
12	74.65 $\pm$ 4.34	56.29 $\pm$ 5.29	48.77 $\pm$ 5.34		
13	75.83 $\pm$ 3.67	54.42 $\pm$ 5.24	47.48 $\pm$ 5.90		
14	75.65 $\pm$ 3.89	54.28 $\pm$ 5.31	47.89 $\pm$ 6.11		
15	75.63 $\pm$ 3.80	54.27 $\pm$ 5.34	47.9 $\pm$ 6.15		
P-value	0.960	0.411	0.164	15	0.001

**Table 6.** The mean and SD values of Dmean (in Gy) for various OARs resulted from the IMRT protocol 14 and 3D-CRT protocol

Protocol	D <sub>mean</sub> $\pm$ SD(Gy) (brain stem)	D <sub>mean</sub> $\pm$ SD(Gy) (spinal cord)	D <sub>mean</sub> $\pm$ SD(Gy) (optic chiasma)	D <sub>mean</sub> $\pm$ SD(Gy) (optic nerves)	D <sub>mean</sub> $\pm$ SD(Gy) (parotid glands)	D <sub>mean</sub> $\pm$ SD(Gy) PTV
IMRT	30.18 $\pm$ 0.96	29.51 $\pm$ 0.98	21.2 $\pm$ 2.37	16.85 $\pm$ 2	32.55 $\pm$ 1.12	69.94 $\pm$ 0.08
3D-CRT	17.26 $\pm$ 1.31	14.54 $\pm$ 1.37	16.44 $\pm$ 2.06	17.25 $\pm$ 1.98	54.77 $\pm$ 1.77	69.86 $\pm$ 0.124
P-value	P<0.001	P<0.001	0.135	0.845	P<0.001	0.680

**Table 7.** NTCP  $\pm$  SD % values of the OARs for the IMRT protocol 14 and 3D-CRT protocol based on relative sterility model for all the NPC patients for different ranges of the common volume between the TPTV and OARs with relevant p-values

OARs	Mean of the TNTCP $\pm$ SD(%) values of the OARs for different ranges of the common volume between the TPTV and OARs			
	Protocol	0 – 6 (cm <sup>3</sup> )	6 – 12 (cm <sup>3</sup> )	$\geq$ 12 (cm <sup>3</sup> )
Brainstem	IMRT	0.01 $\pm$ 0.01	0 $\pm$ 0	0.01 $\pm$ 0.01
	3D-CRT	0.03 $\pm$ 0.01	0.03 $\pm$ 0.01	0.05 $\pm$ 0.01
	p-value	0.339	0.081	0.035
Spinal cord	IMRT	0 $\pm$ 0	0 $\pm$ 0	0 $\pm$ 0
	3D-CRT	0.03 $\pm$ 0.01	0.03 $\pm$ 0.01	0 $\pm$ 0
	p-value	0.104	0.081	-
Optic chiasm	IMRT	0 $\pm$ 0	0 $\pm$ 0	0.06 $\pm$ 0.06
	3D-CRT	0.01 $\pm$ 0.01	0 $\pm$ 0	0 $\pm$ 0
	p-value	0.339	-	0.351
Optic nerves	IMRT	0 $\pm$ 0	0.02 $\pm$ 0.02	0.01 $\pm$ 0.01
	3D-CRT	0 $\pm$ 0	0 $\pm$ 0	0.03 $\pm$ 0.03
	p-value	-	0.347	0.351
Parotid glands	IMRT	19.25 $\pm$ 3	40.09 $\pm$ 5.20	50.63 $\pm$ 4.52
	3D-CRT	37.97 $\pm$ 5.7	70.54 $\pm$ 5.14	76.36 $\pm$ 9.04
	P-value	P < 0.001	P < 0.001	0.005

**Table 8.** TNTCP, TCP and P+  $\pm$  SD % values of the OARs for the IMRT protocol 14 and 3D-CRT protocol based on relative seriality model for all the NPC patients for different ranges of the common volume between the TNTCP and OARs with relevant p-values

Radiobiological parameters	Mean of TNTCP, TCP and P+ values $\pm$ SD (%) for different ranges of the common volume between the TPTV and OARs			
	Protocol	0 – 6 (cm <sup>3</sup> )	6 – 12 (cm <sup>3</sup> )	$\geq$ 12 (cm <sup>3</sup> )
TNTCP	IMRT	18.57 $\pm$ 0.87	40.09 $\pm$ 5.20	45.23 $\pm$ 5.51
	3D-CRT	34.98 $\pm$ 8	64.31 $\pm$ 3.58	69.29 $\pm$ 8.21
	p-value	P < 0.001	P < 0.001	0.01
TCP	IMRT	94.30 $\pm$ 1.83	94.35 $\pm$ 1.46	93.200 $\pm$ 2.01
	3D-CRT	93.20 $\pm$ 1.04	92.86 $\pm$ 1.22	92.62 $\pm$ 1.69
	p-value	0.454	0.489	0.860
P+	IMRT	75.72 $\pm$ 3.86	54.28 $\pm$ 5.29	47.95 $\pm$ 6.93
	3D-CRT	58.27 $\pm$ 8.17	28.53 $\pm$ 3.79	23.32 $\pm$ 6.72
	P-value	P < 0.001	P < 0.001	0.007

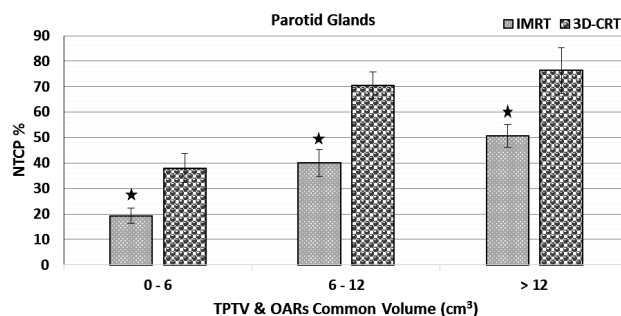


**Figure 2.** The NTCP mean and SD values of parotid glands for the IMRT and 3D-CRT protocols for different ranges of the common volume between the TPTV and OARs. Stars (\*) indicate significant lower NTCP values of the IMRT compared to 3D-CRT protocol and vertical lines represent different ranges of the common volume between the TPTV and OARs.

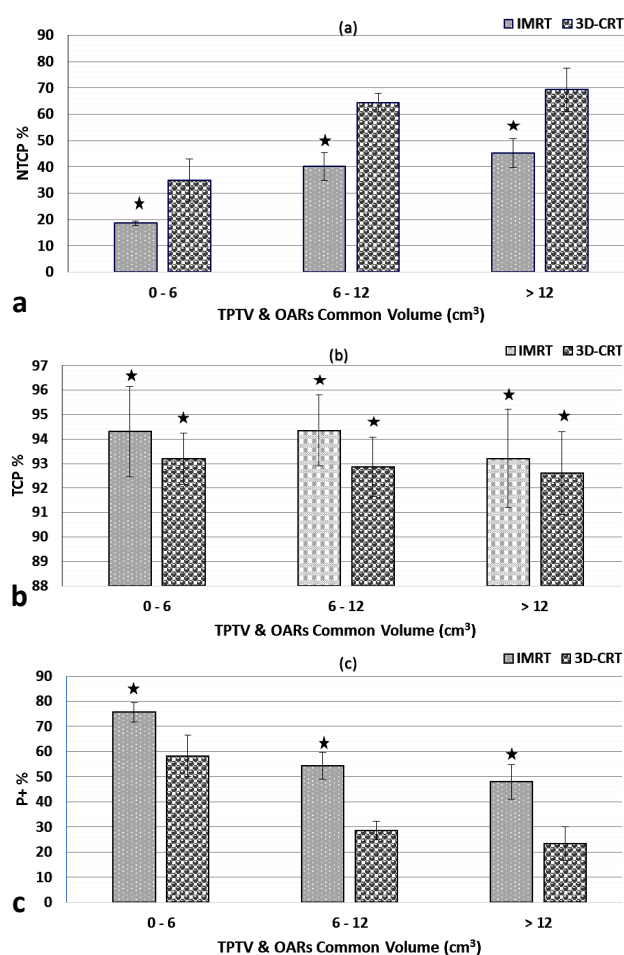


**Figure 3.** The mean of NTCP, TCP, P+ and SD values for the IMRT and 3D-CRT protocols for different ranges of common volume between the TPTV and OARs. Stars (\*) indicate significant lower NTCP and higher P+ values of the IMRT compared to 3D-CRT protocol and vertical lines represent different ranges of the common volume between the TPTV and OARs.

## DISCUSSION

The aim of this study was to evaluate the treatment quality and efficacy of several developed novel IMRT protocols (with varying collimator and couch angles) as well as a 3D-CRT technique based on the NTCP, TCP, P+ radiobiologic parameters on NPC patients. As reported in a previous study <sup>(24)</sup>, some of these IMRT procedures were implemented to spare sensitive OARs for locally advanced NPC patients mostly based on dosimetric parameters. However, in the current study, an overall 15 developed IMRT protocols were conducted to investigate the effect of changing collimator and couch angles for IMRT treatment planning of NPC patients based on radiobiological parameters. Radiobiological assessment of the developed IMRT techniques was proved to be quite effective, as the region of NPC is very small encompassing several OARs wherein any changes in the collimator and couch angle can play a significant role on the NPC treatment quality and efficacy. Our NPC patients included both the early and advanced stages thereof the analysis of the common volumes between the target and OARs were made based on the NTCP, TCP, and P+ radiobiological parameters. Although the results of all the developed IMRT protocols were acceptable, two specific protocols (13 and 14) indicated a significant reduction of the NTCP for lower range of the common volume between the target and OARs.

Given that IMRT is more costly, labor intensive, and time consuming it brings about a question as to whether it is a wise use of resources. Therefore, various 3D-CRT techniques have also been investigated and proposed on NPC patients to spare the spinal cord. However, using such techniques have been reported to be faced with the problems of field matching, using more fields and phases, and high doses for almost all the OARs <sup>(8,10)</sup>. Considering such reasons, we also focused on developing a new 3D-CRT technique for NPC treatment planning and compared it with our developed IMRT protocols. Our developed 3D-CRT technique was based on the fit and shield of spinal cord while avoiding beam junctions, covering the PTV with the highest dose and less number of fields and phases. Some previous studies <sup>(25, 26)</sup> have also been done to compare the 3D-CRT and IMRT planning for NPC patients using radiobiological modeling. However, such studies have not proposed any optimal treatment planning (s) for NPC patients based on their radiobiological parameters (namely TCP, NTCP, and P+) and anatomical relationships between their target and OARs. Furthermore, in previous studies only simple traditional IMRT (without any variation of collimator and couch angles) and 3D-CRT planning procedure have been used and the complication free tumor control probability (p+) has not been reported.

All the patients investigated in our study had a general feature of having a common volume just between the parotid glands and TPTV and no other OARs (brainstem, spinal cord, optic chiasm, and optic nerves). Therefore, a main reason for the increased NTCP mean values observed for our developed 3D-CRT technique can be attributed to the increased doses of parotid glands as they are inevitably located in treatment fields and there is no solution to protect them when treated with 3D-CRT. However, our results indicated a very good control of the tumor for both of our developed IMRT and 3D-CRT protocols. There were also no side effects for other OARs including: brainstem, spinal cord, optic chiasm and optic nerves, as all the NTCP mean values for all the developed IMRT and 3D-CRT protocols were small and acceptable (there was no common volume between these organs and TPTV). As indicated in previous studies <sup>(27, 28)</sup>, randomized trials have shown a reduction in late xerostomia from traditional IMRT compared to CRT techniques resulting in an important improvement of the patients' quality of life. By the way, such studies have generally been made without taking into account the common volumes between the parotid glands and TPTV. Based on the approach used in our study, xerostomia, as the clinical side effect of IMRT and 3D-CRT techniques during the treatment of NPC patients, can be attributed to the increased NTCP mean values of parotid glands due to the increased common volume between these glands and TPTV that could eventually lead to increased risk of xerostomia.

The approach developed and used in our study could be quite useful for selecting appropriate protocol (s) via development of required computer algorithms in common TPSs used for NPC patients with IMRT techniques. This can simply be achieved by considering the anatomical parameters of patients, estimating their NTCP values and using them to compare various IMRT protocols of interest and choose the best one leading to the lowest risk to OARs. From another point of view, whenever just the tumor control has a higher priority, the TCP curve derived from different IMRT protocols according to anatomical parameters can show any significant difference between the protocols and help us to select the most appropriate one. But, whenever both of the tumor control and OARs doses have the same priority, investigating the P+ curve could be regarded as a useful tool to select the most appropriate IMRT protocol that limits more the radiation risk to OARs.

## CONCLUSION

Comparison of our developed IMRT and 3D-CRT protocols indicating the lowest NTCP and P+ mean values for the IMRT for all ranges of the common volume suggests IMRT procedure as a better protocol

to be used for treating the NPC patients although both of the IMRT and 3D-CRT protocols provided good results in term of tumor control. In addition, overall it could be concluded that IMRT techniques are more suitable for treating NPC. However, it should be noted that implementing IMRT require more treatment cost, difficulties in quality assurance, and considerable effects of secondary cancer in OARs following the treatment compared to 3D-CRT. Therefore, in clinical practice, whenever patient's parotid glands are not located in the treatment field or there is a small range (0 to 6 cm<sup>3</sup>) of common volume between parotid glands and TPTV, 3D-CRT technique could be recommended for treating NPC. But, for the patients with higher ranges (6 to 12 and  $\geq 12$  cm<sup>3</sup>) of common volume between parotid glands and TPTV, the IMRT protocols should preferably be recommended to reduce their severe complications of late xerostomia.

## ACKNOWLEDGEMENTS

*This research was carried out at Tarbiat Modares University. The patients' imaging and radiotherapy planning procedures were carried out at Radiotherapy and the Oncology Departments of Shohaday-e-Tajrish hospital, Tehran, Iran. Therefore, the authors express their sincere appreciation to the above institutions for their financial help and technical assistance.*

**Funding:** This research received no specific grant from any funding agency, commercial or not-for-profit sectors.

**Ethical approval statement:** The research project leading to this study was approved by the Research Ethical Committee of Tarbiat Modares University (ID no.: RESEARCH.MODARES.REC.1397.037, date: 16/05/2018).

**Conflict of Interest:** All authors declare no conflict of interest.

**Authors' contributions:** GhS and B H designed the study, radiotherapy plans done by GhS under the supervision of MB, AR contributed in referring the patients and delineating their GTVs, GhS, and BH drafted the manuscript. All authors contributed in the interpretation of data and approved the final manuscript.

## REFERENCES

1. Vokes E, Liebowitz D, Weichselbaum R (1997) Nasopharyngeal carcinoma. *Lancet*, **350**: 1087–1091.
2. Ali H and Al-Sarraf M (2000) Chemotherapy in advanced nasopharyngeal cancer. *J Oncol*, **14**: 1223–1230.
3. Al-Sarraf M, LeBlanc M, Giri PG, Fu K, Cooper J, Vuong T, et al. (1998) Chemoradiotherapy versus radiotherapy in patients with advanced nasopharyngeal cancer: phase III randomized intergroup study 0099. *J Clin Oncol*, **16**: 1310–1317.
4. Lee N, Harris J, Garden AS, Straube W, Glisson B, Xia P, et al. (2009) Intensity modulated radiation therapy with or without chemotherapy for nasopharyngeal carcinoma: radiation therapy oncology group phase II trial 0225. *J Clin Oncol*, **27**: 3684–3690.



5. Sultanem K, Shu H, Xia P, Akazawa C, Quivey J, Verhey L, et al. (2000) Three-dimensional intensity modulated radiotherapy in the treatment of nasopharyngeal carcinoma: the University of California–San Francisco experience. *Int J Radiat Oncol Biol Phys*, **48**: 711–722.
6. Kam M, Suen J, Choi P, Choi P, Teo P (2002) Intensity-modulated radiotherapy in nasopharyngeal carcinoma: dosimetric advantage over conventional plans and feasibility of dose escalation. *Int J Radiat Oncol Biol Phys*, **56**: 145–157.
7. Pow E, Kwong D, McMillan A, Wong M, Sham J, Leung L, et al. (2006) Xerostomia and quality of life after intensity-modulated radiotherapy versus conventional radiotherapy for early-stage nasopharyngeal carcinoma: initial report on a randomized controlled clinical trial. *Int J Radiat Oncol Biol Phys*, **66**: 981–991.
8. Bentel G (1992) Radiation therapy planning. 2nd ed., New York.
9. Coia L, Galvin J, Sontag M, Blitzer P, Brenner H, Cheng E, et al. (1991) Three-dimensional photon treatment planning in carcinoma of the larynx. *Int J Radiat Oncol Biol Phys*, **21**: 183–192.
10. Neve WD, Wagter CD, Jaeger KD, Thienpont M, Colle C, Derycke S, et al. (1996) Planning and delivering high doses to targets surrounding the spinal cord at the lower neck and upper mediastinal levels: Static beam segmentation technique executed with a multileaf collimator. *Radiother Oncol*, **40**: 271–279.
11. Kutcher GJ, Fuks Z, Benner H, Brown A, Burman C, Cheng E, et al. (1991) Three-dimensional photon treatment planning for carcinoma of the nasopharynx. *Int J Radiat Oncol Biol Phys*, **21**: 169–182.
12. Sailer SL, Sherouse GW, Chaney EL, Rosenman J, Tepper J, et al. (1991) A comparison of postoperative techniques for carcinomas of the larynx and hypopharynx using 3-D dose distributions. *Int J Radiat Oncol Biol Phys*, **21**: 767–777.
13. Shon JW, Suh JH, Pohar S (1995) A method for delivering accurate and uniform radiation dosage to the head and neck with asymmetric collimators and a single isocenter. *Int J Radiat Oncol Biol Phys*, **32**: 809–813.
14. Mesbahi A, Rasuli N, Nasiri B, et al. (2017) Radiobiological Model-Based Comparison of Three-Dimensional Conformal and Intensity-Modulated Radiation Therapy Plans for Nasopharyngeal Carcinoma. *IJMP*, **14**: 190–196.
15. Hamatani N, Sumida I, Takahashi Y, Oda M, Seo Y, Isohashi F, et al. (2017) Three-dimensional dose prediction and validation with the radiobiological gamma index based on a relative seriality model for head-and-neck IMRT. *J Radiat Res*, **58**: 701–709.
16. Moretto F, Rampino M, Munoz F, Redda M, Reali A, Balcet V, et al. (2014) Conventional 2D (2DRT) and 3D conformal radiotherapy (3DCRT) versus intensity-modulated radiotherapy (IMRT) for nasopharyngeal cancer treatment. *La radiologia medica*, **119**: 634–641.
17. Sharbo G, Hashemi B, Bakhshandeh M, Rakhsha A (2019) Radiobiological assessment of nasopharyngeal cancer IMRT using various collimator angles and non-coplanar fields. *J Radiother Pract*, 1–8.
18. Li Q, Pei H, Mu J, Hu Q, Hu Q, Gu W (2013) Segment edit and segment weight optimization: two techniques for intensity modulated radiation therapy and their application to the planning for nasopharyngeal carcinoma. *Technol Cancer Res Treat*, **12**: 403–409.
19. White P, Chan KC, Cheng KW, Chan K, Chau M (2013) Volumetric intensity modulated arc therapy vs. conventional intensity-modulated radiation therapy in nasopharyngeal carcinoma: a dosimetric study. *J Radiat Res*, **54**: 532–545.
20. Radiation Therapy Oncology Group. RTOG 0615: a phase II study of concurrent chemoradiotherapy using three – dimensional conformal radiotherapy (3D-CRT) or Intensity – Modulated Radiation Therapy (IMRT) + Bevacizumab (BV) for locally or regionally advanced nasopharyngeal cancer. <http://irochouston.mdanderson.org/RPC/CREDENTIALING/files/0615Master-2-16-11.pdf>. Accessed on the 12<sup>th</sup> November 2020.
21. Niemierko A and Goitein M (1993) Implementation of a model for estimating tumor control probability for an inhomogeneously irradiated tumor. *Radiother Oncol*, **29**: 140–7.
22. Monica W, Lucullus H, Peter K (2014) The use of biologically related model (Eclipse) for the intensity-modulated radiation therapy planning of nasopharyngeal carcinomas. *PLoS ONE*, **9**: e112229.
23. Kallman P, Lind BK, Brahme A (1992) An algorithm for maximizing the probability of complication-free tumour control in radiation therapy. *Phys Med Biol*, **37**: 871–890.
24. Han G, Liu D, Gan H, Denniston KA, Li S, Tan W, et al. (2014) Evaluation of the dosimetric feasibility of hippocampal sparing intensity-modulated radiotherapy in patients with locally advanced nasopharyngeal carcinoma. *PLoS one*, **28**: e90007.
25. Boughalia A, Marcie S, Fellah M, Chami S, Mekki F (2015) Assessment and quantification of patient set-up errors in nasopharyngeal cancer patients and their biological and dosimetric impact in terms of generalized equivalent uniform dose (gEUD), tumour control probability (TCP) and normal tissue complication probability (NTCP). *BJR*, **88**: 20140839.
26. Wang W, Yang H, Mi Y, Hu W, Ding W, Xie, Y, et al. (2015) Rules of parotid gland dose variations and shift during intensity modulated radiation therapy for nasopharyngeal carcinoma. *Radiat Oncol*, **10**: 1–6.
27. Rathod S, Gupta T, Ghosh-Laskar S, Murthy V, Budrukkar A, Agarwal J (2013) Quality-of-life (QOL) outcomes in patients with head and neck squamous cell carcinoma (HNSCC) treated with intensity-modulated radiation therapy (IMRT) compared to three-dimensional conformal radiotherapy (3D-CRT): evidence from a prospective randomized study. *Oral Oncol*, **49**: 634–642.
28. Tribius S and Bergelt C (2011) Intensity-modulated radiotherapy versus conventional and 3D conformal radiotherapy in patients with head and neck cancer: is there a worthwhile quality of life gain? *Cancer treatment reviews*, **37**: 511–519.

